Neurobiology of Aging 124 (2023) 1–10

Contents lists available at ScienceDirect

Neurobiology of Aging

journal homepage: www.elsevier.com/locate/neuaging.org

Brain connectivity in frailty: Insights from The Irish Longitudinal Study on Ageing (TILDA)

Raquel Gutiérrez Zúñiga[a,b,#,*], James R.C. Davis[b,c,#], Rory Boyle[d], Céline De Looze[b,c], James F. Meaney[e], Robert Whelan[a,f,g], Rose Anne Kenny[b,c,h], Silvin P. Knight[a,c], Román Romero Ortuño[a,b,c,h]

[a] Global Brain Health Institute (GBHI), Trinity College Dublin, Dublin, Ireland
[b] The Irish Longitudinal Study on Ageing (TILDA), Trinity College Dublin, Dublin, Ireland
[c] Discipline of Medical Gerontology, School of Medicine, Trinity College Dublin, Dublin, Ireland
[d] Department of Neurology, Massachusetts General Hospital/Harvard Medical School, Boston, MA, USA
[e] Centre for Advanced Medical Imaging (CAMI), St James's Hospital, Dublin, Ireland
[f] Trinity College Institute of Neuroscience (TCIN), Trinity College Dublin, Dublin, Ireland
[g] School of Psychology, Trinity College Dublin, Dublin, Ireland
[h] Mercer's Institute for Successful Ageing (MISA), St James's Hospital, Dublin, Ireland

ARTICLE INFO

Article history:
Received 25 August 2022
Revised 29 December 2022
Accepted 3 January 2023
Available online 7 January 2023

Keywords:
Brain connectivity
Frailty
Connectome-based predictive modeling
Ageing
Magnetic resonance imaging

ABSTRACT

Frailty in older adults is associated with greater risk of cognitive decline. Brain connectivity insights could help understand the association, but studies are lacking. We applied connectome-based predictive modeling to a 32-item self-reported Frailty Index (FI) using resting state functional MRI data from The Irish Longitudinal Study on Ageing. A total of 347 participants were included (48.9% male, mean age 68.2 years). From connectome-based predictive modeling, we obtained 204 edges that positively correlated with the FI and composed the "frailty network" characterised by connectivity of the visual network (right); and 188 edges that negatively correlated with the FI and formed the "robustness network" characterized by connectivity in the basal ganglia. Both networks' highest degree node was the caudate but with different patterns: from caudate to visual network in the frailty network; and to default mode network in the robustness network. The FI was correlated with walking speed but not with metrics of global cognition, reinforcing the matching between the FI and the brain connectivity pattern found (main predicted connectivity in basal ganglia).

1. Introduction

The normal ageing process is characterized by a progressive adaptation of the brain networks to the gradual age-related changes in body and brain organ-systems (Chan et al., 2014). Resting-state functional magnetic resonance imaging (rs-fMRI) can provide important information on spontaneous functional brain connectivity, and in the recent past, this noninvasive method has been used to study how brain networks adapt and change during normal ageing (Wen et al., 2020). Increase in global cooperation between different subsystems (integration), decrease in independent processing in specialized subsystems (segregation) (Chan et al., 2021; Wang et al., 2021) and decrease in connectivity within the default mode (DMN, which is active when resting), salience (which perceives and generates the appropriate response to a stimulus (Menon & Uddin, 2010; Seeley, 2019)), and motor networks are the most frequently reported age-related brain connectivity changes (Wen et al., 2020; Zonneveld et al., 2019). These brain network changes have been associated with cognitive traits; for example, segregation has been found to have a mediating role in the age-related decline of executive functions (Madden et al., 2020).

The ageing process is highly heterogeneous, and notwithstanding overall population-based averages, individuals can be placed on

* Corresponding author at: Global Brain Health Institute, Trinity College Dublin, College Green, Ground Floor, Lloyd Building, Dublin D02 W272, Ireland. Tel.: +353 01 896 4472.
E-mail address: raquel.gutierrezzuniga@gbhi.org (R.G. Zúñiga).
These 2 authors share the first position.

0197-4580/$ – see front matter
https://doi.org/10.1016/j.neurobiolaging.2023.01.001

a continuum from more to less successful ageing, independently of chronological age (Romero-Ortuno & O'Shea, 2013). Frailty (with the opposite being robustness) is a major, potentially modifiable (Dent et al., 2019) determinant of biological age and is defined as a state of physiological vulnerability to stressors due to dysregulation in multiple biological systems (Campbell & Buchner, 1997). Whilst the science around the operationalization of frailty is still evolving (Romero-Ortuño et al., 2021), one of the main approaches in clinical practice and research is the Frailty Index (FI), which is a continuous measure originally proposed by Rockwood and Mitnitski (Rockwood & Mitnitski, 2011) and defines frailty in terms of the degree of accumulation of health deficits at a given chronological age (Searle et al., 2008).

At the intersection between Neuroscience and Gerontology, a study in 2017 in the English Longitudinal Study of Ageing reported that a 47-item FI was independently predictive of incident dementia (Rogers et al., 2017). Although a limitation of that study is that the diagnosis of dementia was self-reported, studies in the Rush Memory and Aging project reported that people who developed dementia or mild cognitive impairment became frailer at a faster pace independently of the neuropathological burden (Wallace et al., 2021), meaning that there may be an inter-relationship between cognition and frailty, but the mechanisms underpinning the reported associations remain obscure. However, new insights could be obtained from functional brain connectivity studies. Some rs-fMRI studies focusing on the term "physio-cognitive decline syndrome" (defined as global cognition being 1.5 standard deviation lower than the same age population) highlighted the importance of connectivity between the hippocampus and cerebellum (Chung et al., 2021). However, another study found that the neurophysiological and brain structural markers of cognitive frailty differ from those of Alzheimer's Disease (Kocagoncu et al., 2022). Moreover, other studies focusing on the physical frailty phenotype described lower activity in the supplementary motor area (Lammers et al., 2020) and lower connectivity between cortical areas relevant for motor tasks (posterior parietal cortex and frontoparietal cortex) without involvement in other cognitive areas (Suárez-Méndez et al., 2020).

With computational advances in recent years, machine learning (ML) methodologies have taken hold in the field of Neuroscience, with the development of algorithms to predict brain connectivity associated with different behavioral and cognitive characteristics from rs-fMRI data (Wein et al., 2021). Connectome-based predictive modeling (CPM) is an ML technique used to identify brain connectivity patterns that predict a defined trait (Shen et al., 2017). CPM has been successfully applied to the study of traits such as creative ability (Beaty et al., 2018), cognitive reserve (Boyle et al., 2021) and fluid intelligence (Finn et al., 2015); however, it had not yet been applied to frailty.

The aim of our study was to contribute new insights into the brain connectivity signatures of frailty by applying CPM to a 32-item self-reported FI using rs-fMRI data available from The Irish Longitudinal Study on Ageing (TILDA). We identified brain connectivity patterns associated with increasing frailty (i.e., higher FI) and increasing robustness (i.e., lower FI). This approach was conducted with a view to gain novel insights into possible mechanisms that may underlie the previously reported associations between different definitions of frailty and brain connectivity.

2. Material and methods

2.1. Setting

TILDA is a prospective cohort study that collects health, economic and social data from a nationally representative sample of community-dwelling adults living in Ireland aged 50 years and over. In wave 1 of the study, TILDA used a sampling strategy that incorporated multistage selection of respondents and geographic clustering of addresses and stratification to reduce sampling error. In summary, the sampling frame was based on the Irish Geodirectory, a comprehensive and up-to-date listing and mapping of all residential addresses in the Republic of Ireland, compiled by An Post (the Irish Postal Service) and Ordnance Survey Ireland. Participants were randomly selected using the RANSAM sampling procedure, so that each residential address in Ireland had an equal probability of selection (Donoghue et al., 2018; Kearney et al., 2011; Whelan & Savva, 2013). In the present study, we utilized data from participants in wave 3 of the study, which took place between March 2014 and December 2015. Of all participants attending the wave 3 health assessment center, a random subset was invited to return for brain MRI at the National Centre for Advanced Medical Imaging (CAMI) at St James's Hospital, Dublin, Ireland (https://www.3tcentre.com/). The inclusion and exclusion criteria for the TILDA MRI substudy have been described elsewhere; briefly, other than participants' refusal to participate, the only a priori exclusion criteria were related with the impossibility to perform the MRI (e.g., due to metallic implants or pacemakers) (Donoghue et al., 2018). So far, Wave 3 of the study is the only one with MRI data (https://tilda.tcd.ie/about/where-are-we-now/).

2.2. MRI data acquisition

TILDA MRI data was obtained using a 3 T Philips Achieva scanner during a 45-minute MRI battery. Rs-fMRI data was acquired using a 6 minute 51.9 second gradient echo-planar imaging (EPI) sequence (flip angle = 90°, slice thickness = 3.2 mm, slice gap = 0.3 mm, number of slices = 38, repetition time (TR) = 2000 ms, time to echo (TE) = 28 ms). Structural MRI data were acquired using a 3D T1 Magnetization Prepared - RApid Gradient Echo (MPRAGE) scan with the following parameters: Field of View (FOV) = 240 × 240 × 162mm, matrix size = 288 × 288 × 180, SENSitivity Encoding (SENSE) = 2, TR = 6.7 ms, TE = 3.1 ms. The voxel size for the rs-fMRI sequences was 3 × 3 × 3.2 mm^3.

2.3. MRI data preprocessing

The MRI data preprocessing procedure has been described in full elsewhere (Boyle et al., 2022). Briefly, functional and structural images were first manually reoriented, then visually inspected for artefacts, data quality issues, possible lesions, and severe atrophy. Images were then preprocessed using SPM12 (Friston, et al., 2006) with a 36-parameter preprocessing pipeline, which includes global signal regression. Rs-fMRI were corrected for slice-timing and head motion. Nuisance regressors consisted of 6 motion estimates, mean white matter (WM) signal, mean cerebrospinal fluid (CSF) signal, and mean global signal, and the derivatives, quadratic terms, and squares of derivatives of these 9 parameters. Normalized functional images and variance images were created and visually inspected for data quality issues, and motion-related issues and artefacts, respectively. Mean framewise displacement (FWD) and other motion metrics were created to identify participants above/below Power et al. criterion of 0.5 mm for mean FWD (Power et al., 2012). Participants were then subject to thresholding such that only those with mean FWD below 0.5 mm were retained. In addition, the participants were also subject to a threshold based on a percentile frame to frame motion. Participants with frame-to-frame motion above the 97.5th percentile were excluded, as per previously published CPM studies (Boyle et al., 2022; Finn et al., 2015; Shen et al., 2017). Finally, data were temporally smoothed with a zero-mean unit-variance Gaussian filter (approximate cut-off frequency of 9.37

Hz) using BioImageSuite. The code used for quality control of the rs-fMRI is available on https://github.com/rorytboyle/fMRI_QC.

2.4. Functional connectivity network construction

As per previous CPM studies (Boyle et al., 2022; Finn et al., 2015), the rs-fMRI data were parcellated according to the Shen 268-node functional atlas (Shen et al., 2013) by re-slicing the preprocessed functional volumes using spm_reslice (SPM12 http://fil.ion.ucl.ac.uk/spm/). Using BioImageSuite, the mean time series for each node was calculated as the average time series across all voxels within each node, for each participant. Functional connectivity between each pair of nodes was calculated by applying Pearson correlation to the average time course between each pair of nodes. The correlation coefficients were normalized by a Fisher z-transformation. This resulted in a 268 × 268 connectivity matrix for each participant in both datasets. The code used for construction of the connectivity matrices is available on https://github.com/rorytboyle/fMRI_connectivity_processing.

2.5. Frailty index

We utilized a self-reported 32-item FI previously operationalized in TILDA as per standard procedure requirements (Roe et al., 2017). Individual items included diagnoses, functional difficulties, sensory impairments, polypharmacy, and other subjective deficits. For each participant, the FI was calculated as the sum of the deficits present divided by 32. This FI is based on the self-completion questionnaires (SCQ) that were sent to participants' homes during the wave 3 data collection period (March 2014–December 2015). MRI appointments were also conducted within the wave 3 collection period, but SCQ and MRI acquisition did not take place during exactly the same time. The 32 FI items are listed in Appendix A. Conscious that some FI items could have very low or zero prevalence (e.g., stroke), we chose to retain all 32 items to help comparability with the same TILDA FI previously derived and validated in the total TILDA sample (Knight et al., 2021; Roe et al., 2017).

2.6. Connectome-based predictive modeling of the Frailty Index

CPM was applied to the dataset in MATLAB. As recommended by (Poldrack et al., 2020; Varoquaux et al., 2017) a repeated k-fold cross-validation (CV) method was employed. In this case, a 10-fold CV was repeated 1000 times. CPM consists of the following steps: edge selection, network strength calculation, model fitting, model application, model evaluation as detailed in Fig. 1. In edge selection, a partial Spearman correlation (adjusted for age, sex, and mean FWD) is performed across all participants in the training fold, between each edge (i.e., brain connection) and the FI. Edges giving rise to statistically significant ($p < 0.01$) correlations are retained via binary masks of equal dimension with a single connectivity matrix (268 × 268): a positive mask for positive correlations and a negative mask for negative correlations. Next, positive and negative network strengths (PNS and NNS) are calculated for each participant by applying the appropriate mask to the connectivity matrix and summing across all selected edges. Using training data, 2 univariate linear models that regress FI on PNS and NNS are fitted. Using the test fold data, the network masks are applied to each connectivity matrix, the networks strengths calculated, and a FI score predicted using the linear models. For each participant 2 FI scores are predicted: 1 using the positive network model (FI_{pos}) and 1 using the negative network model (FI_{neg}). The models were evaluated via comparison of actual versus predicted FI values using Pearson correlation and the mean absolute error (MAE), in line with best-practice guidelines for predictive modeling in neuroimaging (Poldrack et al., 2020). After 1000 iterations, the mean and standard deviation (SD) of the performance metrics is extracted. The significance of the selected edges is assessed via permutation testing in which the CPM procedure is repeated 1000 times (in this case) with the connectivity matrices and outcome variables shuffled (permuted) with respect to each other; the results arising from each permutation are compared to the mean scores and the significance is calculated as $p = \frac{number\ of\ permutation\ scores \leq mean\ score}{1000}$. The code for the CPM is publicly available (code available here: https://github.com/rorytboyle/flexible_cpm), with 2 customizations for our purpose: first, the manual change of the partial correlation method to "Spearman" in the "CPM_fs_relate_partial.m" function script; and second, the extraction of standard deviation values for the sets of 1000 R and MAE results, additional to the "Neuromethods_main_analysis_CPM.m" script.

2.7. Correlation between the Frailty Index and measures of cognitive and physical performance

In view of the 32-item FI being self-reported and including both cognitive and physical items (see Appendix A), and in order to maximize the clinical interpretability of the CPM results, we endeavored to investigate the correlation between the FI and test-based measures of cognitive and physical performance in the included TILDA participants.

Cognitive tests were the Mini-Mental State Examination (Folstein et al., 1975) and the Montreal Cognitive Assessment (Nasreddine et al., 2005) as measures of global cognition (Kenny et al., 2013). These 2 cognitive tests were selected from those available in the TILDA battery because of their frequent use internationally, both in research and clinical practice, as well-validated measures of global cognition Physical performance tests were the timed up-and-go (TUG) (Hartley et al., 2022) and the usual (preferred) gait speed (UGS) (Davis et al., 2021). In the TUG, participants stood up from sitting, walked 3 meters at normal pace along a line on the floor, turned around, walked back to the chair and sat down. The time (in seconds) from "Go" to when participants were seated again was measured with a stopwatch. Gait speed was assessed using a computerized walkway (4.88 m active area) with embedded pressure sensors (GAITRite; CIR Systems Inc., New York, NY). Participants performed 2 walks at usual pace and to avoid inclusion of acceleration and deceleration, starting 2.5 meters before and finishing 2 meters after the walkway. UGS (in m/s) was calculated as the average of 2 consecutive walks.

To explore the associations between the FI and each of the above test-based measures whilst controlling for age (in years), sex (0: male; 1: female), and level of education (none or primary; secondary; third or higher), we computed partial Spearman correlations. This was conducted with IBM SPSS Statistics for Windows, Version 27.0. Armonk, NY: IBM Corp.

2.8. Ethics

Ethical approval was obtained from the Faculty of Health Sciences Research Ethics Committee in Trinity College Dublin, Ireland. Additional ethics approval was received for the MRI sub-study from the St James's Hospital/Adelaide and Meath Hospital, Inc. National Children's Hospital, Tallaght (SJH/AMNCH) Research Ethics Committee, Dublin, Ireland. Written informed consent was obtained from all TILDA participants. Those attending for MRI also signed an additional MRI-specific consent form.

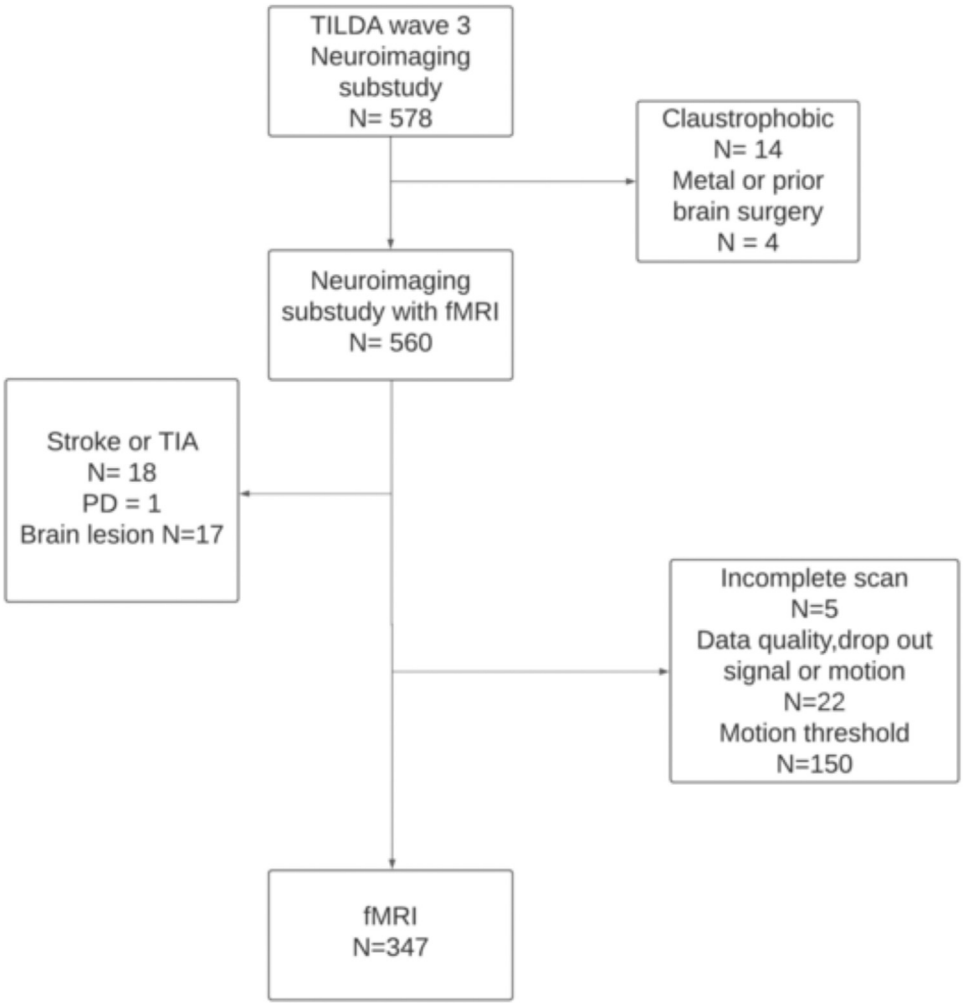

Fig. 1. Flow chart of included participants. Abbreviations: fMRI, functional magnetic resonance imaging; PD, Parkinson disease; TIA, transient ischemic attack. (For interpretation of the references to color in this figure legend, the reader is referred to the Web version of this article.)

3. Results

The flowchart of included participants and full exclusion details is shown in Figure 1. From an initial sample of 560 MRI participants, 32 were excluded due to clinical reasons (history of Parkinson's disease, stroke or the presence of cerebral lesions), and 181 due to rs-fMRI quality issues (incomplete scan, motion and scanner artifacts), leaving a final sample of 347 participants. The mean age of this final cohort was 68.2 years and 48.9% were male. For descriptive purpose, the proportion of those with FI $\geq$ 0.25 was 6.3% (this cut-off has been used to describe clinically significant frailty (Romero-Ortuno, 2013)). Other cohort descriptive are shown in Table 1. The prevalence of each FI item is reported in Appendix A.

From the CPM, we obtained 204 edges that positively correlated with the FI and composed the "frailty network" (R [2SD] = 0.169, [0.029]; p = 0.009; MAE [2SD] = 0.067 [0.001]) selected in at least 9010 CV-folds (CV - folds (k = 10, iterations = 1000 $\therefore$ total CV-folds = 10 $\times$ 1000 = 10,000); and 188 edges that negatively correlated with the FI and formed the "robustness network" (R [2SD] = 0.195, [0.037]; p = 0.006; MAE [2xSD] = 0.066 [0.001]) selected in at least 9022 CV-folds. The FI was used as a continuous variable in the CPM analyses; that means that the frailer a participant was, the higher the probability to have the described brain connectivity pattern; and vice versa.

Table 1
Descriptives of the 347 TILDA participants included in the analyses.

Characteristic	Descriptive
Male; N (%)	169 (48.7)
Age (y); mean (SD); median (IQR)	68.2 (7.2); 68 (65-73)
Education; N (%):	
- None/primary	69 (19.7)
- Secondary	124 (35.7)
- Third/higher	154 (44.4)
Frailty Index; mean (SD); median (IQR)	0.099 (0.08); 0.078 (0.031-0.14)
Frailty Index $\geq$ 0.25; N (%)	22 (6.3)
MMSE score; mean (SD); median (IQR)	28.89 (1.26); 29 (28-30)
MoCA score; mean (SD); median (IQR)	26.01 (2.9); 27 (25-28)
TUG (seconds); mean (SD); median (IQR)	9.01 (1.65); 8.77 (7.97-9.84)
UGS (m/s); mean (SD); median (IQR)	137.61 (18.5); 138.2 (126.8-150.5)

N: number; SD: standard deviation. A Frailty Index $\geq$ 0.25 has been used to dichotomize frailty (Romero-Ortuno, 2013). MMSE: Mini-Mental State Examination; MoCA: Montreal Cognitive Assessment; SART: Sustained Attention to Response Task; TUG: timed up-and-go; UGS: usual gait speed. The sample prevalence of each Frailty Index item is reported in Appendix A, and the distribution of the FI is presented in Appendix B.

For the "frailty network" we found higher connectivity located in the visual system areas (52 significant edges, 25.5% of significant edges) (Fig. 2 A). The projections from the right visual association areas went to both prefrontal cortices and caudate nuclei. The highest degree node was the left caudate (degree 7) (Fig. 2 B),

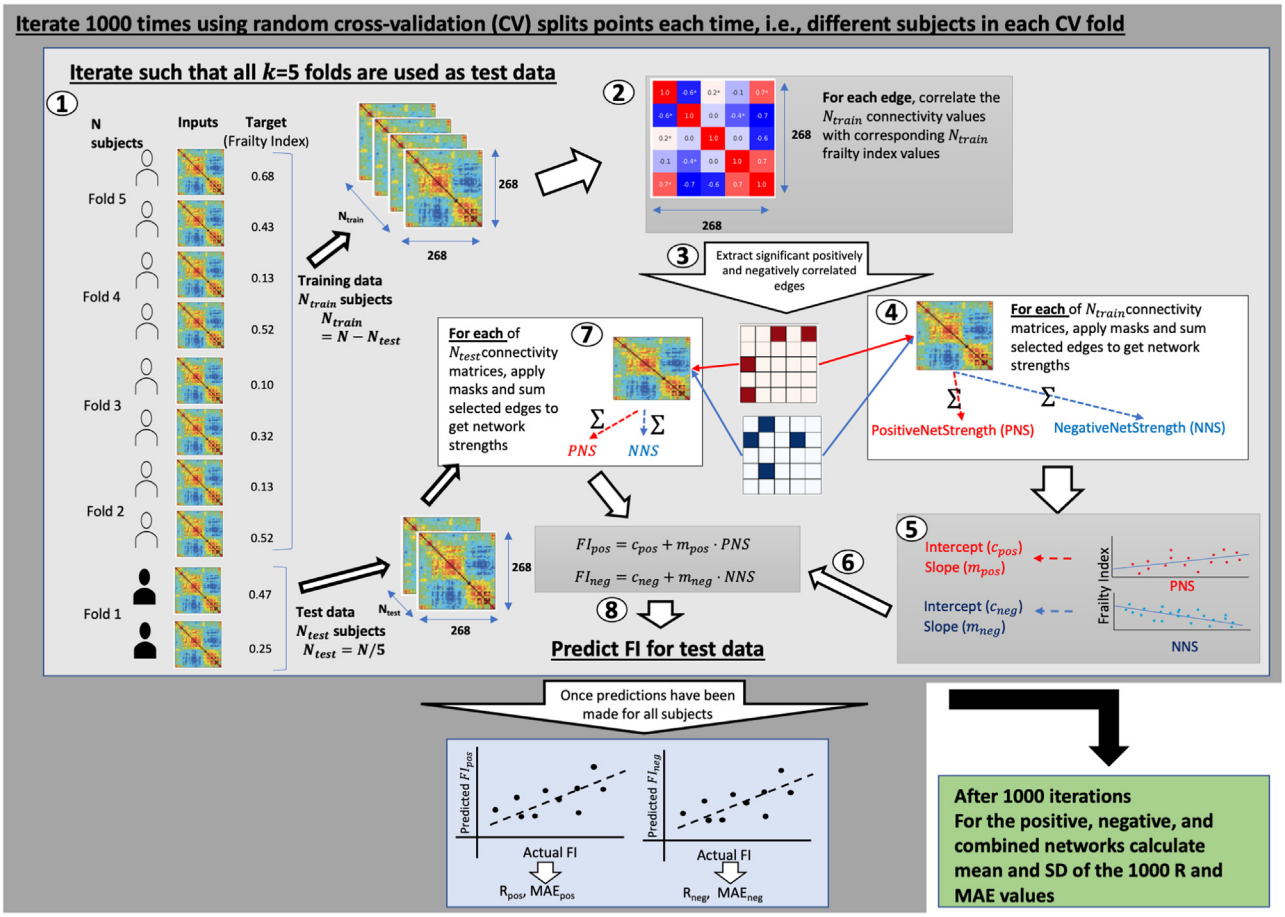

Fig. 2. Schematic representation of the Machine Learning pipeline for the connectome-based predictive modeling of the Frailty Index. Number of folds, number of participants, frailty index values, connectivity matrix images, and scatterplots are all examples to aid the schematic representation and are not representative of the data or results within this paper. Abbreviations: FI, Frailty Index; MAE, mean absolute error; Neg, negative; NNS, negative net strength; PNS, positive net strength; Pos, positive; SD, standard deviation. (For interpretation of the references to color in this figure legend, the reader is referred to the Web version of this article.)

which projected to bilateral visual association areas (BA 19), right secondary visual area (BA 18), right pars opercularis (BA 44) and left medulla (brainstem). All of the connections from the caudate were selected by the model in at least 94.4% of the total number of CV - folds (within 9441 and 10,000 iterations).

The "robustness network" exhibited higher connectivity in the basal ganglia (39 significant edges, 20.7% of significant edges) (Fig. 3A), and from there to both temporal cortices and limbic regions. The highest degree node was the right caudate (degree 6) with projections to dorsal posterior cingulate cortex bilaterally (BA 31), right temporal inferior gyrus (BA 20), left temporal pole (BA 38) and left middle temporal gyrus (BA 21) (Fig. 3B), all of which are default mode network related areas. These connections were selected in at least 93.4% of the total number of CPM CV-folds (10,000).

As regards the associations between the FI and test-based performance measures, UGS was significant after adjusting for age, sex and education level (N = 345, Rho = -0.146, p = 0.008); global cognition (Mini-Mental State Examination: N = 345, Rho = -0.021, p = 0.701; Montreal Cognitive Assessment: N = 344, Rho = -0.004, p = 0.939) was not associated with the FI.

4. Discussion

The aim of our study was to contribute new insights at the intersection between Neuroscience and Gerontology by applying a connectome predictive modeling to a 32-item self-reported Frailty Index in a subcohort of 347 TILDA MRI participants. Results evidenced a "frailty network" that was predominantly characterized by connectivity of the visual network (right more than left). On the other side of the continuum, a "robustness network" was predominantly characterized by connectivity of the basal ganglia. Moreover, both networks' highest degree node was located in the caudate, but with different connectivity pattern: from caudate to visual network in the frailty network; and to DMN-related areas in the robustness network. To our knowledge, this is the first time that a frailty index has been used as the focus trait for a CPM analysis.

Our result that the right visual network had higher connectivity in the frailty network resonates with the study by Zonneveld et al., who reported an increase in connectivity within the visual network especially in older age even when in general there was reduced within-network connectivity in the DMN, the ventral attention network (VAN) and the sensorimotor network (SMN) (Zonneveld et al., 2019). Moreover, in our frailty network the visual areas displayed connectivity to nodes in both prefrontal cortices and caudates. Previous studies demonstrated the relevance of the connectivity between the extrastriate visual cortex (occipital and parietal visual association areas) with the prefrontal cortex and basal ganglia for visual working memory (that is, the brain's ability to construct and hold an internal representation of the environment and compare with external inputs during conscious attention) (Voytek & Knight, 2010).

Our results are also in agreement with previous studies in which frail participants exhibited lower connectivity within cor-

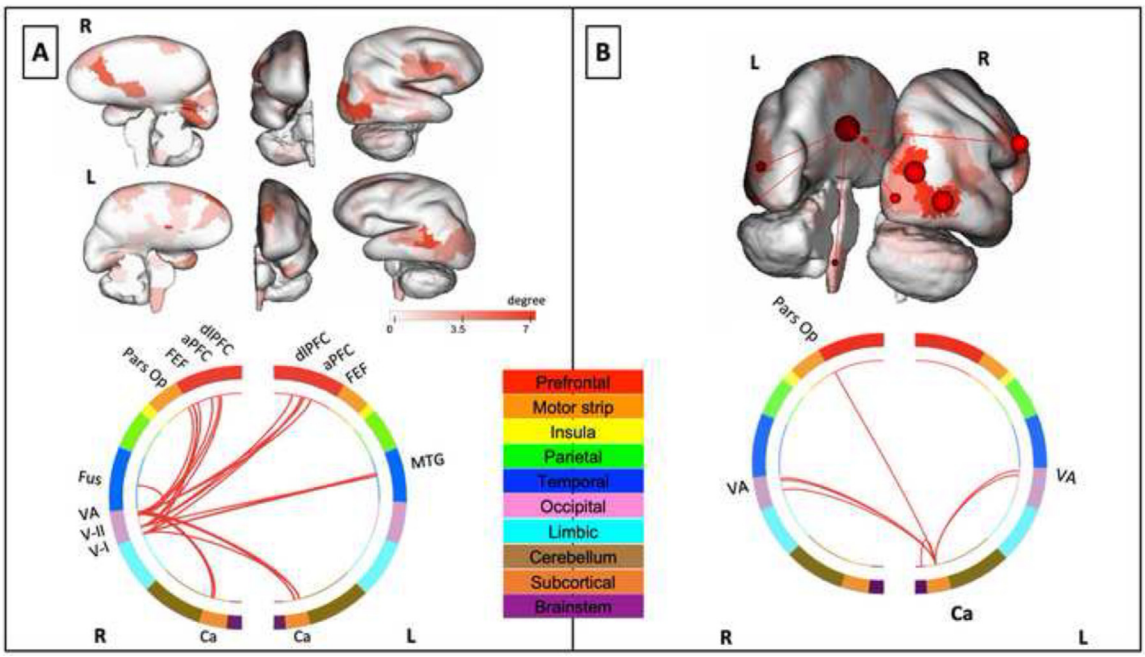

Fig. 3. Connectome-based predictive model for the frailty network. Panel A (left): (top) brain regions implicated in the frailty network and (bottom) the main connectivity from visual association areas to both prefrontal and temporal cortices and caudates. Panel B (right): seed-based conectivity map showing the area with the highest degree and its projections.
Abbreviations: aPFC: anterior prefrontal cortex; Ca, Caudate; Fus, Fusiform gyrus; dlPFC: dorsolateral prefrontal cortex; FEF, frontal eye field; MTG, middle temporal gyrus; Pars Op, pars opercularis; V-I, visual primary; V-II, visual secondary; VA, visual association. (For interpretation of the references to color in this figure legend, the reader is referred to the Web version of this article.)

tical motor relevant areas. Rodríguez-Mañas' group, using seed-based analysis taking the supramarginal gyrus as a seed, found that in frail participants the connectivity with frontoparietal clusters of motor tasks was reduced, together with lower connectivity in the DMN (Suárez-Méndez et al., 2020). Our results are in agreement with previous findings in that in contrast with the robust network, the frailty network exhibited lower connectivity of the motor nucleus with cortical motor relevant areas or DMN areas, but an increase in the connectivity with visual areas that could hypothetically be related with the need for the aid of other networks due to the reduced connectivity with the cortical sensory-motor hubs.

On the other hand, the robustness network exhibited its main connectivity in the subcortical network, with projections to DMN-related areas such as angular gyrus (left), temporal pole (left) and dorsal posterior cingulate cortex (bilateral). The caudate was the highest degree area within the robustness network, but in contrast with the frailty network, it displayed connectivity with both lateral temporal areas and posterior cingulate cortex. Alves et al. described a new neuroanatomical model of the DMN that includes subcortical structures connected to the main cortical hubs of the classic DMN, such as the caudate nuclei (Alves et al., 2019). The DMN is defined as a set of brain regions that are normally co-activated during resting state or whilst performing inner tasks ("mind wandering") and de-activate during externally-oriented tasks (Buckner, 2013). The predicted connectivity within the DMN for robust individuals could reflect their normal, healthy resting state. The capacity to quickly select appropriate responses in predictable behavioral contexts, or to act under "autopilot" behavior, requires the activation of the DMN together with the visual-related cortex to ensure timely and accurate responses (Vatansever et al., 2017). From this evidence, we hypothesize that the connectivity between the basal ganglia and cortical DMN areas in the robust network could reflect robust participants' normal state of DMN-basal ganglia connectivity previously described while resting, in contrast with the frailty network. However, this hypothesis should be confirmed in the future with an independent replication cohort.

The fact that the main connectivity patterns found in both frailty and robustness had their higher degree in the caudate is supported by the fact that in our MRI subsample, the FI was only significantly associated with UGS but not with cognitive or physio-cognitive (TUG) tests. The items that compose our FI are mainly focused on mobility, sensory impairments and chronic diseases, and only few items are dedicated to the self-perception of memory, which could explain the lack of association with cognitive tests after adjustment by age, sex, and education. In addition, the lack of association between cognition and our FI is likely to do with the fact that the TILDA subsample included in our study was cognitively well preserved and with a low proportion of clinically significant frailty. Yet previous studies in the whole TILDA cohort showed consistent results, namely that baseline mobility was not associated (Donoghue et al., 2018) or very weakly associated (Hartley et al., 2022) with cognition at follow-up. This finding is also supported by the brain connectivity pattern found with our definition of frailty (main predicted connectivity in basal ganglia and visual system). Other studies found that cognitively frail adults have different neurophysiological and structural MRI biomarkers than patients with defined mild cognitive impairment and Alzheimer's Disease; and those biomarkers were similar in cognitively frail and normal control participants (Kocagoncu et al., 2022), pointing again that frailty defined by functional difficulties may not be a significant cause of dementia of neurodegenerative type.

Our study has limitations other than the lack of an external cohort validation. Regarding the sample size, in ML analyses it is generally accepted that the higher the numbers, the better. However, in our study the risk of bias due to the sample size is low, as the model includes an iteration test to make the results solid, and the

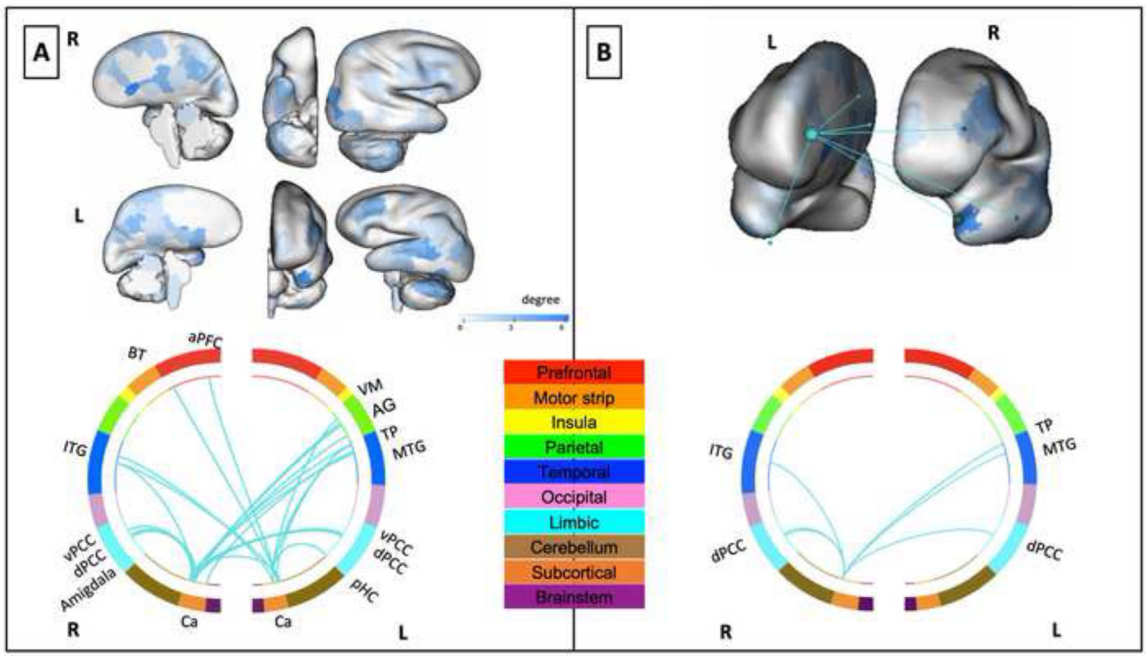

Fig. 4. Connectome-based predictive model for the robustness network. Panel A (left): (top) brain regions implicated in the robustness network and (bottom) main connectivity from caudates to both limbic areas and temporal cortices. Panel B (right): seed-based connectivity map showing the area with the highest degree within the robustness network and its projections.
Abbreviations: AG, angular gyrus; aPFC, anterior prefrontal cortex; BT, broca triangle; Ca, caudate; dPCC, dorsal posterior cingulate cortex; dlPFC, dorsolateral prefrontal cortex; ITG, inferior temporal gyrus; MTG, middle temporal gyrus; TP, temporal pole; VM, visuo motor area; vPCC, ventral posterior cingulate cortex; pHC, parahippocampal area. (For interpretation of the references to color in this figure legend, the reader is referred to the Web version of this article.)

sample is split into training and testing groups with a high number of randomizations. In this TILDA MRI sample, participants were quite homogeneous in terms of age, frailty and cognitive status, with low prevalence's of clinically significant frailty and cognitive impairment, meaning that our results may not be extrapolable to those with more advanced physical and/or cognitive disabilities.

5. Conclusions

Our frailty operationalization (i.e., FI) in our sample of TILDA participants captured a state of impairment of daily physical performance but not significant cognitive impairment. Based on this, CPM results evidenced a "frailty network" that was predominantly characterized by connectivity of the visual network. On the other side of the continuum, a "robustness network" was predominantly characterized by connectivity of the basal ganglia. Moreover, both networks' highest degree node was located in the caudate, but with different connectivity pattern: from caudate to visual network in the frailty network; and to DMN-related areas in the robustness network. Different connectivity patterns along this FI could reflect differences in brain networks' recruitment for the performance of the daily physical tasks. To our knowledge, this is the first time that a CPM model is used to predict frailty with a custom operationalization, opening the door to further research as to how different frailty operationalizations can predict different brain connectivity patterns and be more or less related with cognition, which could help disentangle remaining questions as to how frailty may be implicated in incident cognitive decline.

Verification

The authors declare that the work described has not been published previously (except in the form of an abstract), that it is not under consideration for publication elsewhere.

The manuscript for publication is approved by all authors and tacitly or explicitly by the responsible authorities where the work was carried out, and that, if accepted, it will not be published elsewhere in the same form, in English or in any other language, including electronically without the written consent of the copyright-holder.

TILDA is funded by the Irish Department of Health, Atlantic Philanthropies, and Irish Life. Raquel Gutiérrez-Zúñiga and Roman Romero-Ortuno are funded by the Global Brain Health Institute, Trinity College Dublin. Roman Romero-Ortuno, Silvin Knight and James Davis are also funded by a grant from Science Foundation Ireland 18/FRL/6188. CPM calculations were performed on the Tinney cluster maintained by the Trinity Centre for High Performance Computing (Research IT). This cluster is funded form a Grant from Science Foundation Ireland under Grant number 18/FRL/6188.

Disclosure statement

The authors report no conflicts of interest.

CRediT authorship contribution statement

Raquel Gutiérrez Zúñiga: Conceptualization, Data curation, Formal analysis, Investigation, Methodology, Software, Validation, Visualization, Writing – original draft. **James R.C. Davis:** Data curation, Formal analysis, Investigation, Methodology, Software, Validation, Visualization, Writing – review & editing. **Rory Boyle:** Investigation, Methodology, Software, Writing – review & editing. **Céline De Looze:** Investigation, Methodology, Writing – review & editing. **James F. Meaney:** Data curation, Investigation, Methodology, Resources, Validation, Visualization, Writing – review & editing. **Robert Whelan:** Investigation, Methodology, Writing – review & editing. **Rose Anne Kenny:** Funding acquisition, Investigation, Project administration, Resources, Writing – review & editing.

Silvin P. Knight: Data curation, Investigation, Supervision, Writing – review & editing. **Román Romero Ortuño:** Conceptualization, Funding acquisition, Investigation, Methodology, Project administration, Resources, Supervision, Writing – review & editing.

Appendix A. Thirty-two-item Frailty Index: items and scoring of individual items

Self-reported deficit	Scoring	Prevalence in the cohort (N = 347)
1. Difficulty walking 100 meters	0 = No; 1 = Yes	3; 0.9%
2. Difficulty rising from a chair	0 = No; 1 = Yes	43; 12.4%
3. Difficulty climbing 1 flight of stairs	0 = No; 1 = Yes	10; 2.9%
4. Difficulty stooping, kneeling or crouching	0 = No; 1 = Yes	89; 25.6%
5. Difficulty reaching above shoulder height	0 = No; 1 = Yes	19; 5.5%
6. Difficulty pushing/pulling large objects	0 = No; 1 = Yes	26; 7.5%
7. Difficulty lifting/carrying weights >=10 pounds (4.5 Kg)	0 = No; 1 = Yes	34; 9.8%
8. Difficulty picking up a coin from a table	0 = No; 1 = Yes	9; 2.6%
9. Feeling lonely	0 = None of the time, rarely;	
	0.5 = Some of the time;	19; 5.5%
	1 = All the time	5; 1.4%
10. Self-rated physical health	0 = Excellent, Very good, Good;	
	0.5 = Fair;	21; 6.1%
	1 = Poor	2; 0.6%
11. Self-rated vision	0 = Excellent, Very good, Good;	
	0.5 = Fair;	16; 4.6%
	1 = Poor	5; 1.4%
12. Self-rated hearing	0 = Excellent, Very good, Good;	
	0.5 = Fair;	42; 12.1%
	1 = Poor	5; 1.4%
13. Self-rated day-to-day memory	0 = Excellent, Very good, Good;	
	0.5 = Fair;	52; 15%
	1 = Poor	5; 1.4%
14. Difficulty following a conversation with 4 people	0 = None;	
	0.5 = Some;	71; 20.5%
	1 = Much/Impossible	13; 3.7%
15. Daytime sleepiness	0 = Never, slight chance;	
	0.5 = Moderate chance;	58; 16.7%
	1 = High chance	52; 15%
16. Polypharmacy	0 = No; 1 = Yes	56; 16.1%
17. Knee pain	0 = No; 1 = Yes	13; 3.7%
18. Hypertension	0 = No; 1 = Yes	112; 32.3%
19. Angina	0 = No; 1 = Yes	7; 2%
20. Heart attack	0 = No; 1 = Yes	0; 0%
21. Diabetes	0 = No; 1 = Yes	25; 7.2%
22. Stroke or Transient ischemic attack	0 = No; 1 = Yes	0; 0%
23. High cholesterol	0 = No; 1 = Yes	117; 33.7%
24. Irregular heart rhythm	0 = No; 1 = Yes	13; 3.7%
25. Other cardiovascular disease	0 = No; 1 = Yes	2; 0.6%
26. Cataracts	0 = No; 1 = Yes	49; 14.1%
27. Glaucoma or Age-related macular degeneration	0 = No; 1 = Yes	26; 5.8%
28. Arthritis	0 = No; 1 = Yes	119; 34.4%
29. Osteoporosis	0 = No; 1 = Yes	62; 17.9%
30. Cancer	0 = No; 1 = Yes	14; 4%
31. Varicose ulcer	0 = No; 1 = Yes	8; 2.3%
32. Urinary incontinence	0 = Never, slight chance;	
	0.5 = Moderate chance;	16; 4.6%
	1 = High chance	26; 7.5%

Appendix B. Histogram showing the distribution of the Frailty Index

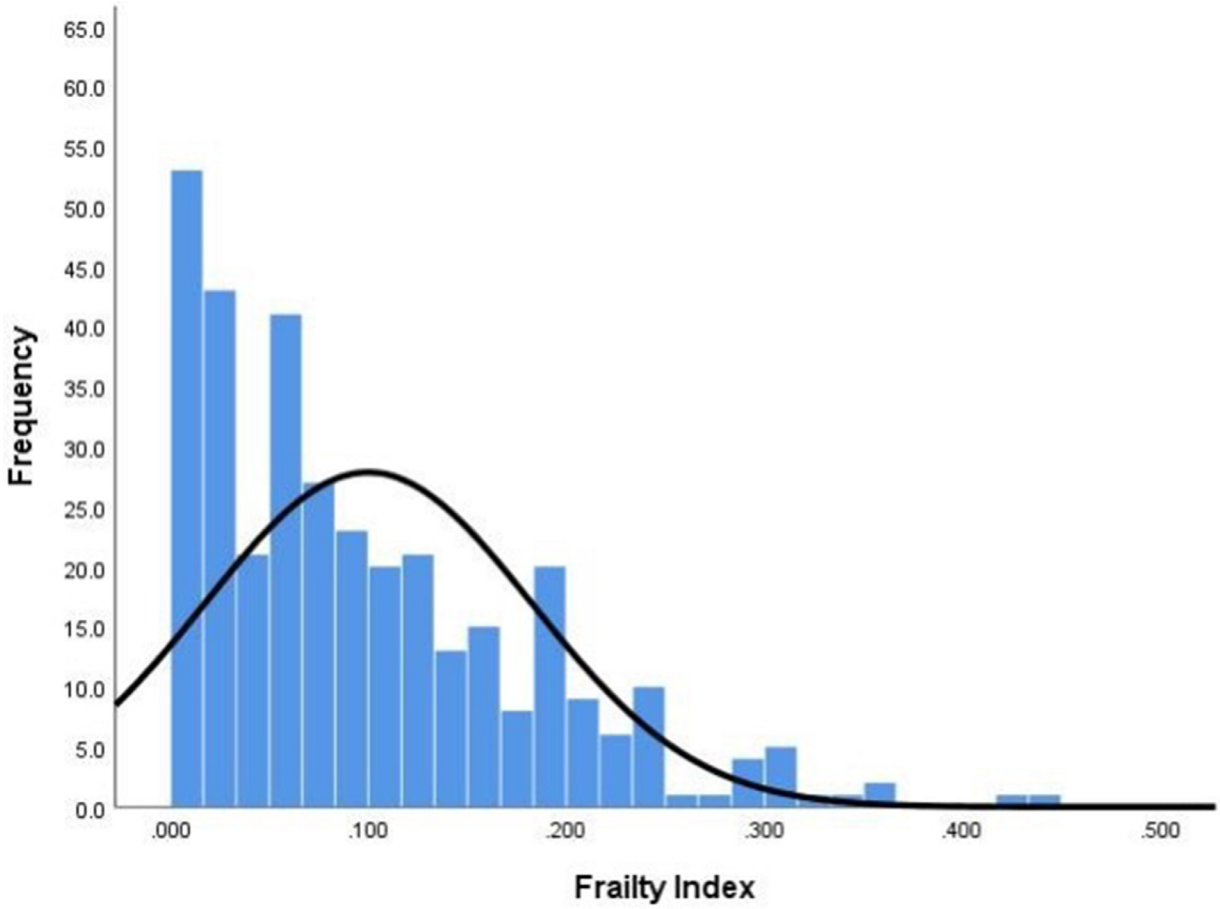

References

Alves, P.N., Foulon, C., Karolis, V., Bzdok, D., Margulies, D.S., Volle, E., Thiebaut de Schotten, M., 2019. An improved neuroanatomical model of the default-mode network reconciles previous neuroimaging and neuropathological findings. Commun. Biol. 2, 1–14. doi:10.1038/s42003-019-0611-3.

Beaty, R.E., Kenett, Y.N., Christensen, A.P., Rosenberg, M.D., Benedek, M., Chen, Q., Fink, A., Qiu, J., Kwapil, T.R., Kane, M.J., Silvia, P.J., 2018. Robust prediction of individual creative ability from brain functional connectivity. Proc. Natl. Acad. Sci. U. S. A. 115, 1087–1092. doi:10.1073/pnas.1713532115.

Boyle, R., Connaughton, M., McGlinchey, E., Knight, S.P., De Looze, C., Carey, D., Stern, Y., Robertson, I.H., Kenny, R.A., Whelan, R., 2021. Connectome-based predictive modeling of cognitive reserve. Alzheimer's Dement 17, 2022. doi:10.1002/alz.057654, 06.01.494342.

Boyle, R., Connaughton, M., McGlinchey, E., Knight, S.P., Looze, C.De, Carey, D., Stern, Y., Robertson, I.H., Kenny, R.A., Whelan, R., 2022. Connectome-based predictive modeling of cognitive reserve using task-based functional connectivity. bioRxiv doi:10.1101/2022.06.01.494342.

Buckner, R.L., 2013. The brain's default network: origins and implications for the study of psychosis. Dialogues Clin. Neurosci. 15, 351–358. doi:10.31887/dcns.2013.15.3/rbuckner.

Campbell, A.J., Buchner, D.M., 1997. Unstable disability and the fluctuations of frailty. Age Ageing 26, 315–318. doi:10.1093/ageing/26.4.315.

Chan, M.Y., Han, L., Carreno, C.A., Zhang, Z., Rodriguez, R.M., LaRose, M., Hassenstab, J., Wig, G.S., 2021. Long-term prognosis and educational determinants of brain network decline in older adult individuals. Nat. Aging 1, 1053–1067. doi:10.1038/s43587-021-00125-4.

Chan, M.Y., Park, D.C., Savalia, N.K., Petersen, S.E., Wig, G.S., 2014. Decreased segregation of brain systems across the healthy adult lifespan. Proc. Natl. Acad. Sci. U. S. A. 111, E4997–E5006. doi:10.1073/pnas.1415122111.

Chung, C.-P., Lee, W.-J., Peng, L.-N., Shimada, H., Tsai, T.-F., Lin, C.-P., Arai, H., Chen, L.-K., 2021. Physio-cognitive decline syndrome as the phenotype and treatment target of unhealthy aging. J. Nutr. Health Aging 25, 1179–1189. doi:10.1007/s12603-021-1693-4.

Davis, J.R., Knight, S.P., Donoghue, O.A., Hernández, B., Kenny, R.A., Romero-ortuno, R., 2021. Comparison of gait speed reserve, usual gait speed, and maximum gait speed of adults aged 50+ in Ireland using explainable machine learning. Front. Netw. Physiol. doi:10.3389/fnetp.2021.754477.

Dent, E., Martin, F.C., Bergman, H., Woo, J., Romero-Ortuno, R., Walston, J.D., 2019. Management of frailty: opportunities, challenges, and future directions. Lancet 394, 1376–1386. doi:10.1016/S0140-6736(19)31785-4.

Donoghue, O., Feeney, J., O'Leary, N., Kenny, R.A., 2018. Baseline mobility is not associated with decline in cognitive function in healthy community-dwelling older adults: findings from the Irish Longitudinal Study on Ageing (TILDA). Am. J. Geriatr. Psychiatry 26, 438–448. doi:10.1016/j.jagp.2017.11.006.

Donoghue, O.A., McGarrigle, C.A., Foley, M., Fagan, A., Meaney, J., Kenny, R.A., 2018. Cohort profile update: the Irish Longitudinal Study on Ageing (TILDA). Int. J. Epidemiol. 47, 1398. doi:10.1093/ije/dyy163, -1398l.

Finn, E.S., Shen, X., Scheinost, D., Rosenberg, M.D., Huang, J., Chun, M.M., Papademetris, X., Constable, R.T., 2015. Functional connectome fingerprinting: identifying individuals using patterns of brain connectivity. Nat. Neurosci. 18, 1664–1671. doi:10.1038/nn.4135.

Folstein, M.F., Folstein, S.E., McHugh, P.R., 1975. Mini-mental state": a practical method for grading the cognitive state of patients for the clinician. J. Psychiatr. Res. 12, 189–198. doi:10.1016/0022-3956(75)90026-6.

Hartley, P., Monaghan, A., Donoghue, O.A., Kenny, R.A., Romero-Ortuno, R., 2022. Exploring bi-directional temporal associations between timed-up-and-go and cognitive domains in the Irish longitudinal study on ageing (TILDA). Arch. Gerontol. Geriatr. 99, 104611. doi:10.1016/j.archger.2021.104611.

Kearney, P.M., Cronin, H., O'Regan, C., Kamiya, Y., Savva, G.M., Whelan, B., Kenny, R.A., 2011. Cohort profile: the Irish Longitudinal study on. Ageing. Int. J. Epidemiol. 40, 877–884. doi:10.1093/ije/dyr116.

Kenny, R.A., Coen, R.F., Frewen, J., Donoghue, O.A., Cronin, H., Savva, G.M., 2013. Normative values of cognitive and physical function in older adults: findings from

the Irish Longitudinal study on ageing. J. Am. Geriatr. Soc. 61. doi:10.1111/jgs.12195.

Knight, S.P., Newman, L., O'connor, J.D., Davis, J., Kenny, R.A., Romero-Ortuno, R., 2021. Associations between neurocardiovascular signal entropy and physical frailty. Entropy 23, 1–19. doi:10.3390/e23010004.

Kocagoncu, E., Nesbitt, D., Emery, T., Hughes, L.E., Henson, R.N., Rowe, J.B., 2022. Neurophysiological and brain structural markers of cognitive frailty differ from Alzheimer's disease. J. Neurosci. 42, 1362–1373. doi:10.1523/JNEUROSCI.0697-21.2021.

Lammers, F., Zacharias, N., Borchers, F., Morgeli, R., Spies, C.D., Winterer, G., 2020. Functional connectivity of the supplementary motor network is associated with Fried's Modified Frailty Score in older adults. J. Gerontol. - Ser. A Biol. Sci. Med. Sci. 75, 2239–2248. doi:10.1093/gerona/glz297.

Madden, D.J., Jain, S., Monge, Z.A., Cook, A.D., Lee, A., Huang, H., Howard, C.M., Cohen, J.R., 2020. Influence of structural and functional brain connectivity on age-related differences in fluid cognition. Neurobiol. Aging 96, 205–222. doi:10.1016/j.neurobiolaging.2020.09.010.

Menon, V., Uddin, L.Q., 2010. Saliency, switching, attention and control: a network model of insula function. Brain Struct. Funct. 214, 655–667. doi:10.1007/s00429-010-0262-0.

Nasreddine, Z.S., Phillips, N.A., Bédirian, V., Charbonneau, S., Whitehead, V., Collin, I., Cummings, J.L., Chertkow, H., 2005. The Montreal Cognitive Assessment, MoCA: a brief screening tool for mild cognitive impairment. J. Am. Geriatr. Soc. 53, 695–699. doi:10.1111/j.1532-5415.2005.53221.x.

Friston, K.J., Ashburner, J., Kiebel, S., Nichols, T., Penny, W., 2006. Statistical Parametric Analysis: The Analysis of Functional Brain Images, 1st ed. Academic Press Inc.

Poldrack, R.A., Huckins, G., Varoquaux, G., 2020. Establishment of Best Practices for Evidence for Prediction: A Review. JAMA Psychiatry 77, 534–540. doi:10.1001/jamapsychiatry.2019.3671.

Power, J.D., Barnes, K.A., Snyder, A.Z., Schlaggar, B.L., Petersen, S.E., 2012. Spurious but systematic correlations in functional connectivity MRI networks arise from subject motion. Neuroimage 59, 2142–2154. doi:10.1016/j.neuroimage.2011.10.018.

Rockwood, K., Mitnitski, A., 2011. Frailty defined by deficit accumulation and geriatric medicine defined by frailty. Clin. Geriatr. Med. doi:10.1016/j.cger.2010.08.008.

Roe, L., Normand, C., Wren, M.A., Browne, J., O'Halloran, A.M., 2017. The impact of frailty on healthcare utilisation in Ireland: Evidence from the Irish longitudinal study on ageing. BMC Geriatr 17, 1–12. doi:10.1186/s12877-017-0579-0.

Rogers, N.T., Steptoe, A., Cadar, D., 2017. Frailty is an independent predictor of incident dementia: evidence from the English Longitudinal Study of Ageing. Sci. Rep. 7. doi:10.1038/s41598-017-16104-y.

Romero-Ortuno, R., 2013. An alternative method for Frailty Index cut-off points to define frailty categories. Eur. Geriatr. Med. 4, 299–303. doi:10.1016/j.eurger.2013.06.005.

Romero-Ortuño, R., Martínez-Velilla, N., Sutton, R., Ungar, A., Fedorowski, A., Galvin, R., Theou, O., Davies, A., Reilly, R.B., Claassen, J., Kelly, Á.M., Ivanov, P.C., 2021. Network physiology in aging and frailty: the grand challenge of physiological reserve in older adults. Front. Netw. Physiol. 1, 1–6. doi:10.3389/fnetp.2021.712430.

Romero-Ortuno, R., O'Shea, D., 2013. Fitness and frailty: opposite ends of a challenging continuum! Will the end of age discrimination make frailty assessments an imperative? Age Ageing 42, 279–280. doi:10.1093/ageing/afs189.

Searle, S.D., Mitnitski, A., Gahbauer, E.A., Gill, T.M., Rockwood, K., 2008. A standard procedure for creating a frailty index. BMC Geriatr 8, 1–10. doi:10.1186/1471-2318-8-24.

Seeley, W.W., 2019. The salience network: a neural system for perceiving and responding to homeostatic demands. J. Neurosci. 39, 9878–9882. doi:10.1523/JNEUROSCI.1138-17.2019.

Shen, X., Finn, E.S., Scheinost, D., Rosenberg, M.D., Chun, M.M., Papademetris, X., Constable, R.T., 2017. Using connectome-based predictive modeling to predict individual behavior from brain connectivity. Nat. Protoc. 12, 506–518. doi:10.1038/nprot.2016.178.

Shen, X., Tokoglu, F., Papademetris, X., Constable, R.T., 2013. Groupwise whole-brain parcellation from resting-state fMRI data for network node identification. Neuroimage 82, 403–415. doi:10.1016/j.neuroimage.2013.05.081.

Suárez-Méndez, I., Doval, S., Walter, S., Pasquín, N., Bernabé, R., Gallo, E.C., Valdés, M., Maestú, F., López-Sanz, D., Rodríguez-Mañas, L., 2020. Functional connectivity disruption in frail older adults without global cognitive deficits. Front. Med. 7, 1–11. doi:10.3389/fmed.2020.00322.

Varoquaux, G., Raamana, P.R., Engemann, D.A., Hoyos-Idrobo, A., Schwartz, Y., Thirion, B., 2017. Assessing and tuning brain decoders: Cross-validation, caveats, and guidelines. Neuroimage 145, 166–179. doi:10.1016/j.neuroimage.2016.10.038.

Vatansever, D., Menon, D.K., Stamatakis, E.A., 2017. Default mode contributions to automated information processing. Proc. Natl. Acad. Sci. U. S. A. 114, 12821–12826. doi:10.1073/pnas.1710521114.

Voytek, B., Knight, R.T., 2010. Prefrontal cortex and basal ganglia contributions to visual working memory. Proc. Natl. Acad. Sci. U. S. A. 107, 18167–18172. doi:10.1073/pnas.1007277107.

Wallace, L.M.K., Theou, O., Godin, J., Ward, D.D., Andrew, M.K., Bennett, D.A., Rockwood, K., 2021. 10-year frailty trajectory is associated with Alzheimer's dementia after considering neuropathological burden. Aging Med 4, 250–256. doi:10.1002/agm2.12187.

Wang, R., Liu, M., Cheng, X., Wu, Y., Hildebrandt, A., Zhou, C., 2021. Segregation, integration, and balance of large-scale resting brain networks configure different cognitive abilities. Proc. Natl. Acad. Sci. 118, 12083–12094. https://doi.org/10.1073/pnas.2022288118

Wein, S., Deco, G., Tomé, A.M., Goldhacker, M., Malloni, W.M., Greenlee, M.W., Lang, E.W., 2021. Brain connectivity studies on structure-function relationships: a short survey with an emphasis on machine learning. Comput. Intell. Neurosci. doi:10.1155/2021/5573740, 2021.

Wen, X., He, H., Dong, L., Chen, J., Yang, J., Guo, H., Luo, C., Yao, D., 2020. Alterations of local functional connectivity in lifespan: A resting-state fMRI study. Brain Behav 10, 1–10. doi:10.1002/brb3.1652.

Whelan, B.J., Savva, G.M., 2013. Design and methodology of the Irish Longitudinal Study on Ageing. J. Am. Geriatr. Soc. 61, 265–268. doi:10.1111/jgs.12199.

Zonneveld, H.I., Pruim, R.H., Bos, D., Vrooman, H.A., Muetzel, R.L., Hofman, A., Rombouts, S.A., van der Lugt, A., Niessen, W.J., Ikram, M.A., Vernooij, M.W., 2019. Patterns of functional connectivity in an aging population: the Rotterdam Study. Neuroimage 189, 432–444. doi:10.1016/j.neuroimage.2019.01.041.